166 *Biochemistry* **2010,** *49,* 166–178
DOI: 10.1021/bi901086v

BIOCHEMISTRY
including biophysical chemistry & molecular biology
Article

Cell Membrane Expression of Cardiac Sodium Channel $Na_v1.5$ Is Modulated by α-Actinin-2 Interaction[†]

Rahima Ziane,[‡] Hai Huang,[‡] Behzad Moghadaszadeh,[∥] Alan H. Beggs,[∥] Georges Levesque,[§] and Mohamed Chahine*,[‡]

[‡]*Centre de Recherche Université Laval Robert-Giffard, and* [§]*Centre de Recherche du CHUL (CHUQ), Unité de Neurosciences, Université Laval, Quebec City, QC, Canada, and* [∥]*Division of Genetics and Program in Genomics, Children's Hospital Boston, Harvard Medical School, 320 Longwood Avenue, Boston, Massachusetts 02115*

Received June 26, 2009; Revised Manuscript Received November 25, 2009

ABSTRACT: Cardiac sodium channel $Na_v1.5$ plays a critical role in heart excitability and conduction. The molecular mechanism that underlies the expression of $Na_v1.5$ at the cell membrane is poorly understood. Previous studies demonstrated that cytoskeleton proteins can be involved in the regulation of cell surface expression and localization of several ion channels. We performed a yeast two-hybrid screen to identify $Na_v1.5$-associated proteins that may be involved in channel function and expression. We identified α-actinin-2 as an interacting partner of the cytoplasmic loop connecting domains III and IV of $Na_v1.5$ ($Na_v1.5$/LIII−IV). Co-immunoprecipitation and His_6 pull-down assays confirmed the physical association between $Na_v1.5$ and α-actinin-2 and showed that the spectrin-like repeat domain is essential for binding of α-actinin-2 to $Na_v1.5$. Patch-clamp studies revealed that the interaction with α-actinin-2 increases sodium channel density without changing their gating properties. Consistent with these findings, coexpression of α-actinin-2 and $Na_v1.5$ in tsA201 cells led to an increase in the level of expression of $Na_v1.5$ at the cell membrane as determined by cell surface biotinylation. Lastly, immunostaining experiments showed that α-actinin-2 was colocalized with $Na_v1.5$ along the Z-lines and in the plasma membrane. Our data suggest that α-actinin-2, which is known to regulate the functional expression of the potassium channels, may play a role in anchoring $Na_v1.5$ to the membrane by connecting the channel to the actin cytoskeleton network.

Muscular contraction and neuronal firing are physiological responses to voltage-gated sodium channel activation in excitable tissues. $Na_v1.5$[1] is the major voltage-sensitive sodium channel in the heart and is responsible for the normal electrical excitability and conduction of the cardiomyocytes. Mutations in the *SCN5A* gene encoding the $Na_v1.5$ protein are associated with several arrhythmogenic syndromes, including long QT syndrome, Brugada syndrome, conduction disorders, sudden infant death syndrome, and dilated cardiomyopathy (*1*, *2*).

$Na_v1.5$ is a transmembrane protein consisting of a single pore-forming α-subunit and several auxiliary β-subunits. Recent studies showed that $Na_v1.5$-associated proteins modulate not only $Na_v1.5$ activity but also its biosynthesis, localization, and/or degradation (*3*). For example, the β_1 and β_2 subunits interact with other proteins and stabilize channel density within the plasma membrane (*4*). In addition, the β_1 and β_3 subunits may enhance the trafficking efficiency of sodium channels in the endoplasmic reticulum (*5*, *6*). Besides the β-subunits, adapter proteins such as syntrophin, dystrophin, and ankyrin have also been shown to participate in the targeting and stabilization of skeletal and cardiac sodium channels at the cell membrane (*7*−*9*), while the ubiquitine-protein ligase (Nedd4-2) acts on $Na_v1.5$ by decreasing channel density at the cell membrane (*3*). Despite this variety of accessory proteins, the precise composition and role of the cardiac sodium channel complex remain poorly understood. It is logical to predict that many more proteins are involved in the dynamic networks of protein−protein interactions with $Na_v1.5$. Here, we describe a novel binding partner of the cardiac sodium channel, α-actinin-2.

α-Actinins belong to a superfamily of F-actin cross-linking proteins that includes spectrin and dystrophin. The four known α-actinin isoforms are encoded by four separate genes (*10*). All four isoforms are 100 kDa, rod-shaped molecules that form antiparallel dimers composed of an N-terminal actin-binding domain, four central spectrin-like repeat motifs (SRM), and a C-terminal calponin homology domain (CH) (*11*). α-Actinins perform a number of important physiological functions, many of which involve binding interactions with other proteins. They link various transmembrane proteins to the actin filament network (*12*−*14*), regulate K^+ channel activity (*15*), and help to maintain cytoskeleton organization (*16*). We performed a yeast two-hybrid screen using LIII−IV as bait to screen a human

[†]This study was supported by grants from the Heart and Stroke Foundation of Quebec (HSFQ) and the Canadian Institute of Health Research (CIHR, MT-13181). M.C. is an Edwards Senior Investigator (Joseph C. Edwards Foundation). B.M. and A.H.B. were supported by Grant R01-AR44345 from the National Institute of Arthritis and Musculoskeletal and Skin Diseases of the National Institutes of Health (NIH) and by Grant 3971 from the Muscular Dystrophy Association. Confocal microscopy was performed at the Children's Hospital Mental Retardation and Developmental Disabilities Research Center Imaging Core with funding from NIH Grant P30 HD18655.

*To whom correspondence should be addressed: Centre de Recherche Université Laval Robert-Giffard, local F-6539, 2601 chemin de la Canardière, Quebec City, QC, Canada G1J 2G3. Telephone: (418) 663-5747, ext. 4723. Fax: (418) 663-8756. E-mail: mohamed.chahine@phc.ulaval.ca.

[1]Abbreviations: $Na_v1.5$, cardiac voltage-gated sodium channel; *SCN5A*, cardiac voltage-gated sodium channel gene; CH, calponin homology domain; SRM, spectrin-like repeat motifs; EF, EF-hand domain; LIII−IV, $Na_v1.5$/LIII−IV.

 Published on Web 11/27/2009

heart cDNA library. Among the partners that we identified, we specifically investigated α-actinin-2. We provide evidence that $Na_v1.5$ binds to the central spectrin rod domain of α-actinin-2. Moreover, we explored the physiological role of α-actinin-2 by the coexpression of α-actinin-2 and $Na_v1.5$ in tsA201 cells, a mammalian cell line. Our results show that α-actinin-2 is a partner for $Na_v1.5$, which may directly or indirectly modulate channel expression and function.

MATERIALS AND METHODS

Yeast Two-Hybrid Plasmid Constructs. The yeast two-hybrid bait vector was obtained using Gateway recombination cloning technology (Invitrogen). The full-length LIII−IV (amino acids 1471−1523) was amplified by PCR from the pcDNA1-$Na_v1.5$ vector. The PCR product was recombined into the pDEST32 vector (Invitrogen) by an LR reaction, resulting in translational fusions between the open reading frame and the GAL4 DNA binding domain. Full-length LIII−IV and full-length α-actinin-2 (amino acids 1−894) constructs were also recombined in the pGBKT7 and pGADT7 vectors and expressed as fusion proteins with a GAL4 DNA binding domain and a GAL4 activation domain, respectively (Matchmaker, Clontech). All the constructs were verified by sequencing.

Mammalian Expression Constructs. The coding segment of human $Na_v1.5$ was cloned into the HindIII and XbaI sites of pcDNA1 (Invitrogen) (*17*). The His_6-LIII−IV fusion protein construct and the pcDNA3-V5-tagged $Na_v1.5$ vector were kindly provided by C. Ahern (Jefferson Medical College, Philadelphia, PA). The human sodium channel β_1 subunit and $Na_v1.8$ channel were constructed in the piRES vector (Invitrogen). The cDNA encoding the calponin hand domain (amino acids 1−86) of human α-actinin-2 was generated by PCR from a pcDNA3-α-actinin-2 vector (kindly provided by D. Fedida, University of British Columbia, Vancouver, BC) and subcloned into the EcoRI and EcoRV sites of pcDNA3.1 (Invitrogen) in frame with the NH_2-terminal Xpress epitope. Five cDNA fragments encoding C-terminally truncated α-actinin-2 [pcDNA3-α-actinin-2/SPEC1 (amino acids 1−390), pcDNA3-α-actinin-2/SPEC2 (amino acids 1−505), pcDNA3-α-actinin-2/SPEC3 (amino acids 1−626), and pcDNA3-α-actinin-2/SPEC4 (amino acids 1−739)] and pcDNA3-Xpress tagged-2 CH domain were generated by introducing stop codons into specific regions of the α-actinin-2 gene. Full-length human α-actinin-1, -3, and -4 cDNAs were used as previously described (*11*). All constructs were sequenced prior to use.

Yeast Two-Hybrid Screen. The two-hybrid screen was performed in yeast strain MaV203 (MATα; *leu*2−3,112; *trp*1−901; *his*3Δ200; *ade*2−101; *cyh*2R; *can*1R; *gal*4Δ; *gal*80Δ; *GAL*1::*lac*Z; $HIS3_{UAS\text{-}GAL1}$::*HIS*3@*LYS*2; *SPAL*10::*URA*3) containing HIS3, LacZ, and URA reporter genes under the control of the GAL4-activating sequences. Briefly, after assessing self-activation and determining the basal expression of the HIS3 reporter gene, we transformed the bait plasmid pDEST32/LIII−IV into yeast strain MaV203 together with a cDNA library prepared from human heart in prey vector pPC86 (Invitrogen) using the lithium acetate method. Candidate clones were selected by plating cotransformants on selective medium lacking tryptophan, leucine, and histidine (−TLH) and supplemented with 10 mM 3-amino-1,2,4-triazole. The clones were confirmed by induction of the URA reporter gene, which allowed growth on synthetic dropout media lacking leucine, tryptophan, and uracil. Plasmids were isolated from candidate clones, and retransformation assays were conducted to verify the interactions using the Matchmaker yeast two-hybrid protocol (Clontech). The selected plasmids were sequenced, and the insert sequences obtained were subjected to BLAST searches.

Cell Culture and DNA Transfection. tsA201 cells, a mammalian cell line derived from human embryonic kidney HEK293 cells by stable transfection with SV40 large T antigen, were grown in high-glucose DMEM supplemented with fetal bovine serum (10%), L-glutamine (2 mM), penicillin G (100 units/mL), and streptomycin (10 mg/mL) (Gibco BRL Life Technologies) in a 5% CO_2 humid atmosphere incubator. In the cotransfection experiments, the DNA ratios of the two plasmids were adjusted to yield approximately equal amounts of expressed proteins. For the patch-clamp experiments, the transfections were performed according to the method of Margolskee et al. (*18*), with a few modifications.

Co-Immunoprecipitation (Co-IP) Assay. Because neither α-actinin-2 nor $Na_v1.5$ is endogenously expressed in tsA201 cells, the cells were transfected with both α-actinin-2 and $Na_v1.5$ cDNA using the calcium phosphate method. The transfections were conducted using 80% confluent cells in a 10 cm plate. The cells were harvested and lysed in STEN buffer [50 mM Tris (pH 7.5), 150 mM NaCl, and 1% (v/v) Triton X-100] supplemented with complete mini EDTA-free protease inhibitors (Roche Diagnostics). The cell lysates were clarified by centrifugation at 15000*g* for 30 min. Equal volumes (500 μL) of cell lysates were incubated with a polyclonal rabbit anti-III−IV loop (2 μg) (Upstate) overnight at 4 °C. Protein G cross-linked to agarose beads (40 μL) (Calbiochem) was added, and the incubation was continued for an additional 4 h. After a quick centrifugation at 5000*g*, the pellet was rinsed five times with STEN buffer to eliminate nonspecific binding. We eluted the immune complexes by boiling the samples for 5 min in reducing sample buffer [0.5 M Tris-HCl (pH 6.8), 20% glycerol, 10% SDS, 0.1% bromophenol blue, and 5% β-mercaptoethanol], separated them via SDS−PAGE, and transferred them onto a polyvinylidene fluoride (PVDF) membrane (Millipore). The membrane was probed with an anti-α-actinin-2 "4B" antibody, and the protein signal was visualized by enhanced chemiluminescence according to the manufacturer's instructions (Amersham Biosciences). For reciprocal co-IP, a rabbit polyclonal anti-α-actinin-2 antibody was used for the immunoprecipitation and the anti-LIII−IV antibody was used for the Western blot analysis. A similar procedure was followed to study the interaction between the α-actinin isoforms and $Na_v1.5$ by coexpressing V5-tagged $Na_v1.5$ with either α-actinin-1, α-actinin-3, or α-actinin-4 in tsA201 cells. The α-actinin isoforms were immunoprecipitated with an anti-V5 antibody (Invitrogen), and the blots were probed with the respective primary antibody (anti-α-actinin-1 "3A3", anti-α-actinin-3 "5A3", or anti-α-actinin-4 "6A3"). For the immunoprecipitation analysis of α-actinin and sodium channel isoforms in native tissue, frozen stripped mouse brain, heart, and skeletal muscle were ground to a fine powder in liquid nitrogen. The powders were further homogenized in STEN lysis buffer using five strokes of a glass homogenizer. The lysates were incubated on ice for 30 min and then microcentrifuged for 15 min at 4 °C. The cell lysates were precleared on protein G beads for 30 min at 4 °C prior to the IP analysis. Equal volumes of supernatants were incubated with 2 μg of anti-LIII−IV antibody and 40 μL of protein G beads for 4 h at 4 °C. After being extensively

washed, the immunoprecipitates were resolved by SDS−PAGE and transferred to PVDF membranes. The membranes were immunoblotted with either the anti-α-actinin-2 antibody, the anti-α-actinin-3 antibody, or the anti-LIII−IV antibody. Lysates were also immunoprecipitated with rabbit preimmune IgG (negative control).

Immunoblots. Cell lysates and immunoprecipitated proteins were separated via 10% SDS−PAGE and transferred to PVDF membranes in transfer buffer (150 mM glycine, 20 mM Tris base, and 20% methanol) for 2 h at 4 °C. The blots were blocked with 5% nonfat skim milk in TBST (50 mM Tris-HCl, 150 mM NaCl, and 0.1% Tween 20) and then incubated with the appropriate primary antibodies [anti-III−IV loop (1:500), anti-V5 (1:5000), anti-α-actinin-1 (1:1000), anti-α-actinin-2 (1:20000), anti-α-actinin-3 (1:1000), anti-α-actinin-4 (1:1000) (*19*), and anti-Xpress (1:5000, Invitrogen)] in blocking buffer for 1 h at room temperature (RT). After three washes with TBST, the blots were incubated with HRP-conjugated goat anti-rabbit antibody or HRP-conjugated goat anti-mouse antibody (1:10000) (Jackson ImmunoResearch Laboratories) for 1 h at RT. The proteins were visualized using an enhanced chemiluminescence detection system (Amersham Bioscience).

Expression and Purification of the His_6 Fusion Protein. Recombinant His_6-LIII−IV fusion protein (amino acids 1471−1523) was transformed into XL1-Blue competent cells (Stratagene). An overnight culture was diluted (1:50) in fresh Luria-Bertani broth, grown to an A_{600} of 0.5, and induced with 1 mM isopropyl β-D-thiogalactopyranoside (Sigma) for 7 h at 37 °C. An XL1-Blue pellet of cells harboring the His_6-LIII−IV fusion protein was resuspended in 200 mM Tris (pH 8), 300 mM NaCl, and 10 mM imidazole supplemented with an EDTA-free complete protease inhibitor mixture (Roche Applied Science) and sonicated six times for 2 s. The bacterial lysate was then centrifuged at 10000*g* for 30 min, and the supernatant was applied to Ni^{2+}-NTA columns (Qiagen) according to the manufacturer's instructions.

Blot Overlay Assay. The interaction between the His_6-LIII−IV fusion protein and α-actinin-2 was assayed using blot overlay assays. tsA201 cells were transiently transfected with increasing amounts (15−45 μg) of cDNA encoding α-actinin-2. Twenty-four hours post-transfection, the cells were washed twice with PBS and lysed in STEN buffer. The cell homogenates were clarified by centrifugation at 15000*g* for 30 min at 4 °C. Equal volumes of whole cell lysates were subjected to SDS−PAGE and blotted onto PVDF membranes. The blots were blocked in 4% nonfat dry milk in Tris-buffered saline supplemented with 0.1% Tween 20 (TBST) overnight at 4 °C, incubated with either 5 mL of 1 μg/mL purified His_6-LIII−IV fusion protein or 5 mL of 1 μg/mL bovine serum albumin (Sigma) in TBST containing 5% skim milk for 90 min at RT, washed three times with TBST, incubated at RT with the polyclonal anti-LIII−IV antibody, washed three times with TBST, and then incubated with HRP-conjugated anti-rabbit antibody. After six washes with TBST, the bands were visualized by ECL. Untransfected tsA201 cells (Unt) and bovine serum albumin protein (BSA) were used as negative controls.

His Pull-Down Assay. The His pull-down assay was performed using the purified His_6-LIII−IV fusion protein to pull down full-length α-actinin-2 or C-terminally truncated α-actinin-2 fragments, which were then detected by specific antibodies. Briefly, the His_6-LIII−IV fusion protein was purified on a Ni^{2+}-NTA column, and 2 μg of purified His_6-LIII−IV fusion protein was bound to Ni^{2+}-NTA beads in PBS for 4 h with rotation. The beads were washed twice for 10 min in PBS containing 0.1% Triton X-100 and once in STEN buffer. The washed beads were incubated with equal volumes (500 μL) of tsA201 cell lysates expressing full-length α-actinin-2 or C-terminally truncated α-actinin-2 proteins in STEN buffer for 1 h at RT. The complexes were centrifuged and extensively washed with 200 mM Tris (pH 8), 300 mM NaCl, and 20 mM imidazole to prevent nonspecific binding. Bound proteins were eluted with the same buffer containing 250 mM imidazole. The samples were then boiled for 5 min in reducing sample buffer and analyzed by Western blotting using the corresponding antibodies. tsA201 cell lysates expressing α-actinin-2 or its C-terminally truncated fragments were also incubated with Ni^{2+}-NTA beads alone as a negative control.

Biotinylation of Cell Surface Proteins. Cell surface proteins were isolated using Pinpoint Cell Surface Protein Isolation kits based on the manufacturer's protocol (Pierce). The $Na_v1.5$ channel was transfected into tsA201 cells together with an empty vector (mock) or increasing amounts (1.5−5 μg) of cDNA encoding α-actinin-2. Forty-eight hours post-transfection, the cells were washed three times with PBS and then incubated with 10 mL of a freshly prepared EZ-Link Sulfo-NHS-SS-Biotin solution in PBS for 30 min at 4 °C with intermittent mixing. This reagent is cell membrane-impermeable and does not label an overexpressed intracell protein (β-tubilin), which was used as a negative control for this assay. The reaction was ended by the addition of 500 μL of quenching solution, and the cells were washed twice with TBS [25 mM Tris-HCl (pH 7.2) and 150 mM NaCl]. The cells were lysed in 500 μL of lysis buffer containing protease inhibitors, sonicated, and incubated on ice for 30 min, to isolate the biotinylated proteins. The clarified cell lysates were incubated with an immobilized NeutrAvidin gel for 1 h at RT by end-over-end mixing. Unbound proteins were removed by three washes with TBS containing protease inhibitors. The biotinylated proteins prebound to the NeutrAvidin gel were eluted using SDS−PAGE sample buffer containing 50 mM DTT for 1 h at RT. $Na_v1.5$ channels in total cell lysates and streptavidin precipitates were analyzed by Western blotting using an anti-LIII−IV antibody. Total cell lysates were also probed for the Na^+/K^+-ATPase α1 subunit, a plasma membrane marker (positive control). To confirm that the biotinylation reagent did not leak into the cell and label intracell proteins, we stripped and reprobed the same blot using an anti-β-tubulin antibody (1:10000; E7, DSHB).

Sodium Current Recordings. The macroscopic sodium currents of transfected tsA201 cells were recorded using the whole-cell configuration of the patch-clamp technique as previously described (*20*). Briefly, patch electrodes were made from 8161 Corning borosilicate glass and coated with Sylgard (Dow-Corning) to minimize their capacitance. Patch-clamp recordings were taken using low-resistance electrodes (< 1 MΩ). Routine series resistance compensation using an Axopatch 200 amplifier (Molecular Devices) was performed to values of $> 80\%$ to minimize voltage-clamp errors. Voltage-clamp command pulses were generated by a microcomputer using pCLAMP version 8.0 (Molecular Devices). Sodium currents were filtered at 5 kHz, digitized at 10 kHz, and stored on a microcomputer equipped with an AD converter (Digidata 1300, Molecular Devices). The data were analyzed using a combination of pCLAMP version 9.0 (Molecular Devices), Microsoft Excel, and SigmaPlot for Windows version 8.0 (SPSS Inc., Chicago, IL).

Immunohistochemistry. The primary antibodies used were rabbit anti-$Na_v1.5$ (Sigma-Aldrich) raised against a purified peptide (DRLPKSDSEDGPRALNQLSC) and monoclonal anti-sarcomeric α-actinin (clone EA53) (Sigma-Aldrich). The secondary antibodies used were Alexa Fluor 488 goat anti-rabbit IgG and Alexa Fluor 594 goat anti-mouse IgG (Invitrogen). A human adult cardiac ventricle autopsy specimen was snap-frozen and cut into 10 μm sections, which were fixed in methanol. The slides were blocked in 10% fetal bovine serum for 30 min and then incubated with primary antibodies [anti-$Na_v1.5$ and anti-α-actinin (1:70)] for 2 h at RT. After three 5 min washes in PBS, the slides were incubated with secondary antibodies (1:200) for 30 min at RT, washed again in PBS, and mounted using Vectashield hardset mounting medium with DAPI (to counterstain nuclei) (Vector Laboratories). The immunolabeled cryosections were examined using an LSM 510 META two-photon confocal microscope (Carl Zeiss AG). Argon and helium/neon lasers were used to detect Alexa Fluor 488 and 594, respectively. DAPI was detected using a two-photon chameleon laser. Twenty-two 0.45 μm serial optical sections were produced with a 2048 × 2048 pixel resolution. For colocalization quatification, two slides labeled with both primary antibodies and only one secondary antibody each were used to threshold confocal images for green ($Na_v1.5$) and red (sarcomeric α-actinin-2) fluorescence. Then the same conditions for staining and imaging were applied to doubly labeled slides stained with both primary and both secondary antibodies. Colocalization coefficients were calculated by deviding the number of colocalized pixels by the total number of either red or green pixels that were above the background threshold. In all images, the measurements were based on regions of interest drawn around individual myocytes that did not contain autofluorescent lipofuscin deposits. Images were analyzed and processed using LSM image (Carl Zeiss AG) and Adobe Photoshop CS version 2.0 (Adobe Systems).

RESULTS

α-Actinin-2 Was Identified as a Candidate Protein That Interacts with $Na_v1.5$ Using a Yeast Two-Hybrid Screen. LIII−IV (amino acids 1471−1523) was used as bait to screen a human heart cDNA library for candidate proteins involved in the regulation of $Na_v1.5$ function using the yeast two-hybrid method (Figure 1A). After screening 10^6−10^7 clones, we isolated four positive clones, which are listed in Table I of the Supporting Information. Most clones were excluded as false positives as they were derived from mitochondrial DNA or because the encoded peptides were out of frame with the GAL4 activation domain. One of the positive clones encoded a 2 kb cDNA fragment of human cardiac α-actinin-2 (GenBank accession number NM-001103). The α-actinin-2 clone comprised amino acids 388−887, including part of the SRM and the Ca^{2+} binding domain. To determine the specificity of the protein interaction, LIII−IV and full-length α-actinin-2 were subcloned as fusion constructs with either the Gal-4 DNA binding domain (BD) in the pGBKT7 vector or the Gal-4 DNA activating domain (AD) in the pGADT7 vector. AH109 yeast cells were then cotransformed with both constructs. The empty DNA binding domain (pGBKT7-empty) and the activation domain (pGADT7-empty) vectors were used as negative controls. All the transformants grew on synthetic complete medium lacking leucine and tryptophan (−TL), indicating that they carried the bait and prey plasmids (Figure 1B, top panel). In contrast, yeast cotransformed

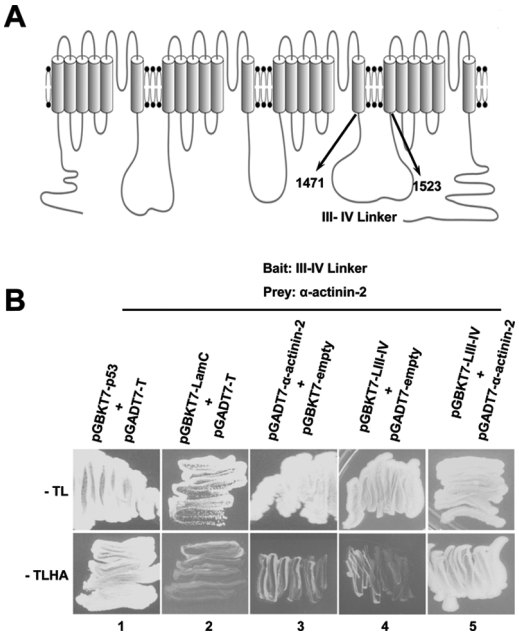

FIGURE 1: Yeast two-hybrid screens of a human heart cDNA library identified α-actinin-2 as a binding partner of the $Na_v1.5$/LIII−IV region. (A) Transmembrane topology of the $Na_v1.5$ α-subunit showing the four homologous domains, each of which is composed of six membrane-spanning segments. The location of the III−IV linker (LIII−IV), which was used as bait, is indicated by the arrows. The numbers correspond to the amino acid positions. (B) α-Actinin-2 was isolated from a yeast two-hybrid screen and subcloned into the pGADT7 vector (pGADT7-α-actinin-2). To confirm the interaction between LIII−IV/BD and α-actinin-2/AD, the AH109 yeast strain was cotransformed with pGBKT7-LIII−IV and -bait constructs with pGADT7-α-actinin-2 and -prey or pGADT7-empty vector as negative controls. p53 (pGBKT7-p53) and SV40 large T-antigen (pGADT7-T) cotransformants were used as positive controls, whereas lamin C (pGBKT7-LamC) and pGADT7-T cotransformants were used as negative controls. The viability of the isolated clones and controls was assessed on medium that lacked tryptophan and leucine (−TL) (cotransformed cells survive) and on counter-selective medium that lacked tryptophan, leucine, histidine, and adenine (−TLHA) (only yeast cells with an interaction between bait and prey proteins survived). The interaction was monitored by histidine and adenine prototrophy. Yeasts cotransformed with either the positive control (pGBKT7-p53 and pGADT7-T) or pGBKT7-LIII−IV and pGADT7-α-actinin-2 grew on the −TLHA plate (bottom panel, lanes 1 and 5). This experiment was repeated four times with similar results.

with either the positive control (Figure 1B, bottom panel, lane 1) or the $Na_v1.5$/LIII−IV and an α-actinin-2 plasmid (Figure 1B, bottom panel, lane 5) grew more efficiently on synthetic complete medium lacking tryptophan, leucine, histidine, and adenine (−TLHA) than yeast cotransformed with either the negative or empty vector controls (Figure 1B, bottom panel, lanes 2−4, respectively). These results demonstrated that the α-actinin-2 prey and the $Na_v1.5$/LIII−IV bait are not self-activating (Figure 1B, bottom panel, lanes 3 and 4, respectively) and that α-actinin-2 and the $Na_v1.5$/LIII−IV bait physically interact in yeast, leading to the activation of a reporter gene (Figure 1B, bottom panel, lane 5). In contrast, the N-terminal region and the cytoplasmic I−II loop of $Na_v1.5$ did not interact with α-actinin-2 (Figure I of the Supporting Information).

α-Actinin-2 Associates with $Na_v1.5$ in Cotransfected tsA201 Cells. To determine whether $Na_v1.5$ and α-actinin-2 associate with one another, co-immunoprecipitations (Co-IP) were employed to determine whether an antibody against one

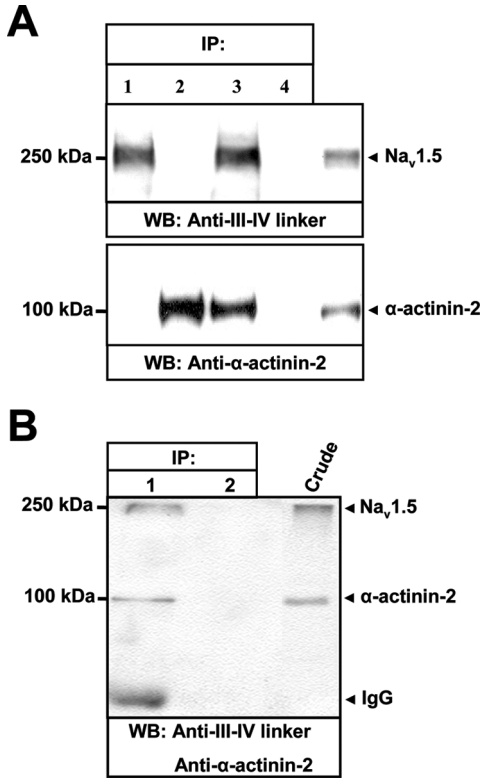

FIGURE 2: α-Actinin-2 and Na$_v$1.5 interacted in mammalian cells. (A) tsA201 cells were transiently transfected with Na$_v$1.5 alone (positive control, lane 1), α-actinin-2 alone (positive control, lane 2), or both (lane 3). The cells were solubilized, and the lysates were immunoprecipitated (IP) with anti-LIII−IV (IP, 1 and 3) or anti-α-actinin-2 antibody (IP, 2) and immunoblotted (IB) with either anti-LIII−IV (top panel) or anti-α-actinin-2 antibody (bottom panel). The anti-LIII−IV antibody immunoprecipitated α-actinin-2 in tsA201 cells coexpressing both proteins (lane 3) but not in tsA201 cells transfected with α-actinin-2 alone (negative control, lane 4). (B) Reciprocal co-immunoprecipitation with the α-actinin-2 antibody for immunoprecipitation and anti-LIII−IV and anti-α-actinin-2 antibodies for Western blotting. tsA201 cells expressing α-actinin-2 and Na$_v$1.5 (lane 1) or Na$_v$1.5 alone (lane 2) were immunoprecipitated with anti-α-actinin-2 antibody (IP, 1 and 2), and the blots were probed with anti-LIII−IV and anti-α-actinin-2 antibodies. The α-actinin-2 antibody (lane 1), but not an irrelevant control antibody (lane 2), specifically co-immunoprecipitated Na$_v$1.5, indicating a bona fide interaction between α-actinin-2 and Na$_v$1.5. The crude extracts represent the cell lysates probed with anti-LIII−IV and anti-α-actinin-2 antibodies and show Na$_v$1.5 and α-actinin-2 levels comparable to those in the sample used for the IP experiment. The arrows indicate the main immunoprecipitation bands. This experiment was repeated three times with similar results.

component, either anti-LIII−IV or anti-α-actinin-2, would co-precipitate the other component. tsA201 cells were cotransfected with constructs for both components. Lysates of transfected cells were co-immunoprecipitated and analyzed for Na$_v$1.5 and α-actinin-2 by immunoblotting (Figure 2A). tsA201 cells were also transfected with the Na$_v$1.5 (lane 1) or α-actinin-2 (lane 2) constructs alone (positive controls). When protein extracts of these cells were immunoprecipitated with either anti-LIII−IV (IP, 1) or anti-α-actinin-2 (IP, 2) antibodies and analyzed by Western blotting with the anti-LIII−IV (top panel) or anti-α-actinin-2 (bottom panel) antibody, the only detectable band, in both cases, was the component that had been transfected. However, when the lysates of the tsA201 cells cotransfected with Na$_v$1.5 and α-actinin-2 were immunoprecipitated with the anti-LIII−IV antibody (IP, 3), there were both Na$_v$1.5

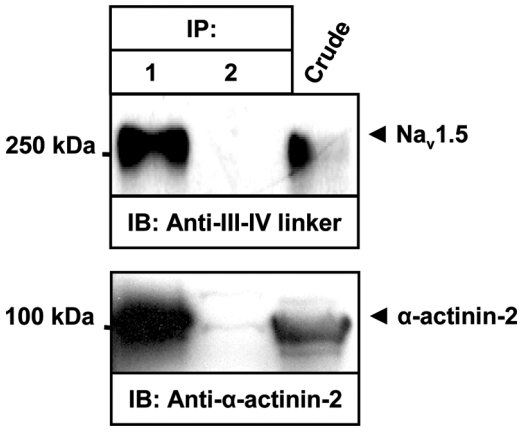

FIGURE 3: Co-immunoprecipitation of α-actinin-2 and Na$_v$1.5 in mouse heart tissue. (A) Proteins were extracted from adult mouse heart in STEN buffer and subjected to immunoprecipitation analysis using either rabbit anti-III−IV loop antibody (LIII−IV) (lane 1) or nonspecific rabbit IgG (lane 2) as described in Materials and Methods. Extracts (Crude) and/or immunoprecipitates (IP) were analyzed by SDS−PAGE and immunoblotted (IB) using either anti-LIII−IV antibody (top panel) or anti-α-actinin-2 antibody (bottom panel). Lysate from heart homogenate (Crude) was used as the positive control. The IgG negative control in lane 2 excluded binding of nonspecific α-actinin-2 to the Na$_v$1.5 channel.

(top panel, lane 3) and α-actinin-2 (bottom panel, lane 3) bands on the blots. Cells transfected with α-actinin-2 alone were used as a negative control. No bands were detected when the negative control lysate was immunoprecipitated with the anti-LIII−IV antibody (lane 4). Reciprocal immunoprecipitation experiments confirmed that Na$_v$1.5 bound to α-actinin-2. As shown in Figure 2B, the α-actinin-2 antibody efficiently immunoprecipitated Na$_v$1.5 in lysates from tsA201 cells cotransfected with Na$_v$1.5 and α-actinin-2 (lane 1) but not in lysates from tsA201 cells transfected with Na$_v$1.5 alone (lane 2). These results demonstrated that full-length Na$_v$1.5 is capable of interacting with full-length α-actinin-2 in mammalian cells.

α-Actinin-2 Associates with Na$_v$1.5 in Cardiac Tissue. To assess the physiological relevance of the α-actinin-2 and Na$_v$1.5 interaction further, a co-immunoprecipitation experiment on mouse cardiac homogenate and double immunolabeling on human cardiac muscle tissue were performed. Using soluble extracts from mouse heart, which had been shown by Western blotting to contain both α-actinin-2 and Na$_v$1.5 proteins (Figure 3), the anti-III−IV linker antibody could co-immunoprecipitate a band at ~100 kDa, which was detected using an anti-α-actinin-2 antibody (Figure 3, bottom panel, lane 1). This band did not appear when an irrelevant rabbit IgG was used for immunoprecipitation (Figure 3, bottom panel, lane 2), showing that the reaction was specific and that α-actinin-2 interacts with Na$_v$1.5 *in vivo*.

α-Actinin-2 Isoforms Bind Na$_v$1.5 in Mammalian Cells. Because of the high degree of identity between α-actinin isoforms (*21*), we investigated the interaction between α-actinin isoforms and Na$_v$1.5 using an experimental setup similar to the one described above. Figure 4 shows that α-actinin-1, α-actinin-3, and α-actinin-4 were able to bind to Na$_v$1.5 (Figure 4A−C, lane 1). Mouse preimmune IgG (Figure 4A−C, lane 2) did not immunoprecipitate α-actinin isoforms from tsA201 cells cotransfected with Na$_v$1.5 and the α-actinin isoforms (α-actinin-1, α-actinin-3, or α-actinin-4) (negative control).

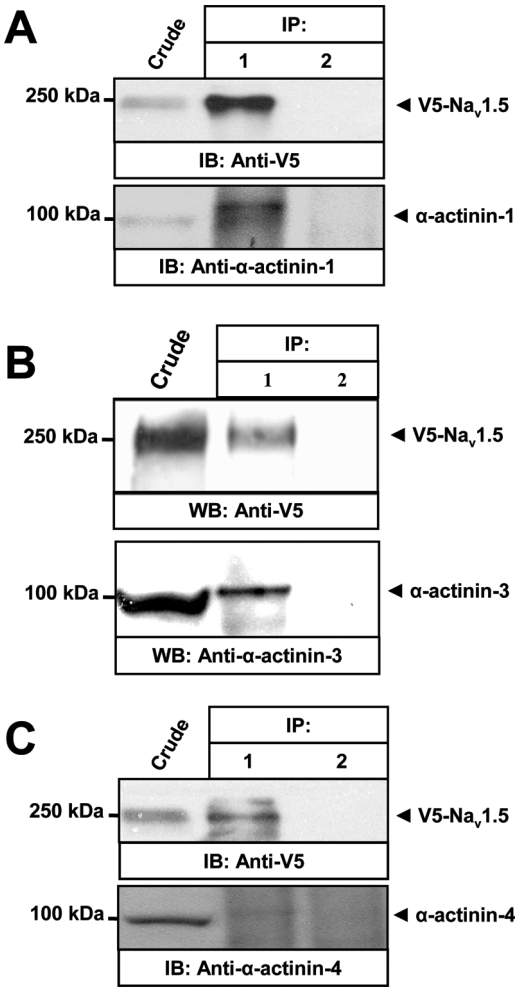

FIGURE 4: α-Actinin isoforms and Na$_v$1.5 interacted in a heterologous expression system. (A) tsA201 cells were transfected with V5-tagged Na$_v$1.5 (V5−Na$_v$1.5) and α-actinin-1 and homogenized in lysis buffer. The cell lysates were immunoprecipitated with anti-V5 antibody (IP, 1) or mouse preimmune serum (negative control) (IP, 2). The blots were probed with anti-V5 antibody (top panel) or anti-α-actinin-1 antibody (bottom panel). The V5 antibody precipitated α-actinin-1 from tsA201 cells cotransfected with V5−Na$_v$1.5 and α-actinin-1 (lane 1) but not the preimmune serum (lane 2). (B) The V5 antibody, but not the preimmune serum (bottom panel, lane 2), immunoprecipitated α-actinin-3 from tsA201 cells cotransfected with V5−Na$_v$1.5 and α-actinin-3 (bottom panel, lane 1). (C) The V5 antibody, but not the preimmune serum (bottom panel, lane 2), immunoprecipitated α-actinin-4 from tsA201 cells transiently expressing Na$_v$1.5 and α-actinin-4 (bottom panel, lane 1). These experiments were repeated three times with similar results.

α-*Actinin-2 Binds Directly to the LIII−IV Region of Na$_v$1.5 in Vitro*. Recombinant proteins were used in blot overlay and histidine pull-down (His pull-down) assays to verify the interaction between α-actinin-2 and Na$_v$1.5 *in vitro* (Figure 5). tsA201 cells were transiently transfected with increasing amounts (15−45 μg) of cDNA encoding α-actinin-2. Twenty-four hours later, the transfected cells were lysed and the cell extracts were separated by SDS−PAGE and blotted onto PVDF membranes. The blots were incubated with either purified His$_6$-LIII−IV fusion protein or BSA (negative control). Binding of His$_6$-LIII−IV fusion protein to α-actinin-2 was revealed by immunoblotting using the anti-LIII−IV antibody. As shown in Figure 5A, His$_6$-LIII−IV fusion protein bound to α-actinin-2 (top panel, lanes 1−3), while no binding was detected in untransfected tsA201 cells (top panel, lane 4) or blot overlays

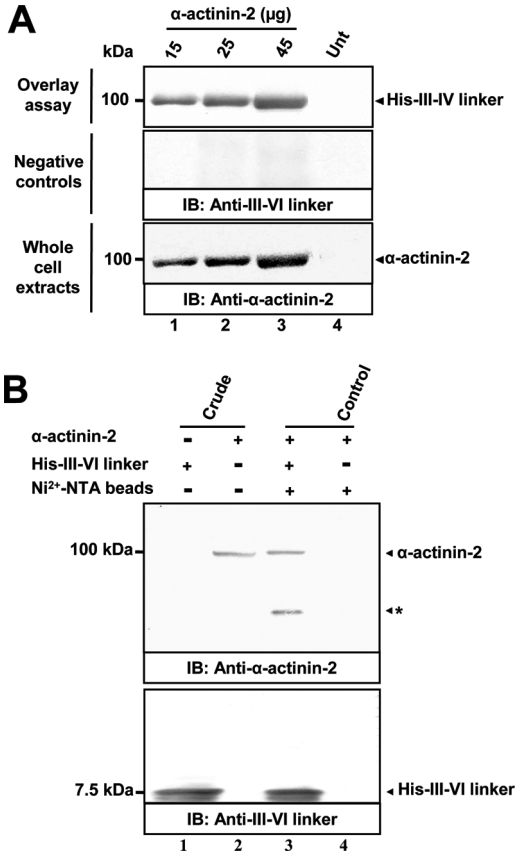

FIGURE 5: α-Actinin-2 and Na$_v$1.5/LIII−IV interacted *in vitro*. (A) Blot overlay assay showing the *in vitro* interaction of α-actinin-2 with the His$_6$-LIII−IV fusion protein. Increasing amounts (15, 25, and 45 μg) of cDNA encoding α-actinin-2 transiently expressed in tsA201 cells were separated by SDS−PAGE and transferred to PVDF membranes. The blots were used to detect the expression of α-actinin-2 proteins (whole cell extracts, bottom panel) or were incubated with either 1 μg/mL purified LIII−IV fusion protein (overlay assay, top panel) or 1 μg/mL BSA (negative control, middle panel) followed by anti-LIII−IV (top and middle panels) or anti-α-actinin-2 antibody (bottom panel). The LIII−IV fusion protein bound specifically to α-actinin-2 in a dose-dependent manner (top panel, lanes 1−3). No binding was detected in the control lane containing extracts from untransfected tsA201 cells (top panel, lane 4) or in the blot incubated with BSA (middle panel). (B) A His pull-down experiment was performed as described in Materials and Methods. tsA201 cell extracts transiently expressing α-actinin-2 were incubated with either His$_6$-LIII−IV fusion protein prebound to Ni^{2+}-NTA beads or Ni^{2+}-NTA beads alone (negative control). After being extensively washed, bound proteins were eluted and separated via 10% SDS−PAGE which were then blotted with anti-α-actinin-2 antibody (top panel) or anti-LIII−IV antibody (bottom panel): lanes 1 and 2, extract starting material; lane 3, His$_6$-LIII−IV fusion protein retained from extract; and lane 4, Ni^{2+}-NTA beads alone (negative control). The asterisk indicates that the band detected in lane 3 may be a degradation product of the His$_6$-LIII−IV fusion protein. These experiments were repeated four times with similar results.

incubated with BSA (middle panel, lanes 1−4). These results suggest that the His$_6$-LIII−IV protein binds specifically to α-actinin-2 in a dose-dependent manner. To further confirm this interaction, His pull-down experiments were conducted (Figure 5B). In the first attempt, His$_6$-LIII−IV protein was expressed in *Escherichia coli*, purified, and immobilized on nickel (Ni^{2+}-NTA) beads (lane 1). The tsA201 cell extracts transiently expressing α-actinin-2 (lane 2) were incubated with either His$_6$-LIII−IV protein prebound to Ni^{2+}-NTA beads (lane 3) or Ni^{2+}-NTA beads alone (lane 4). The extracts were separated by

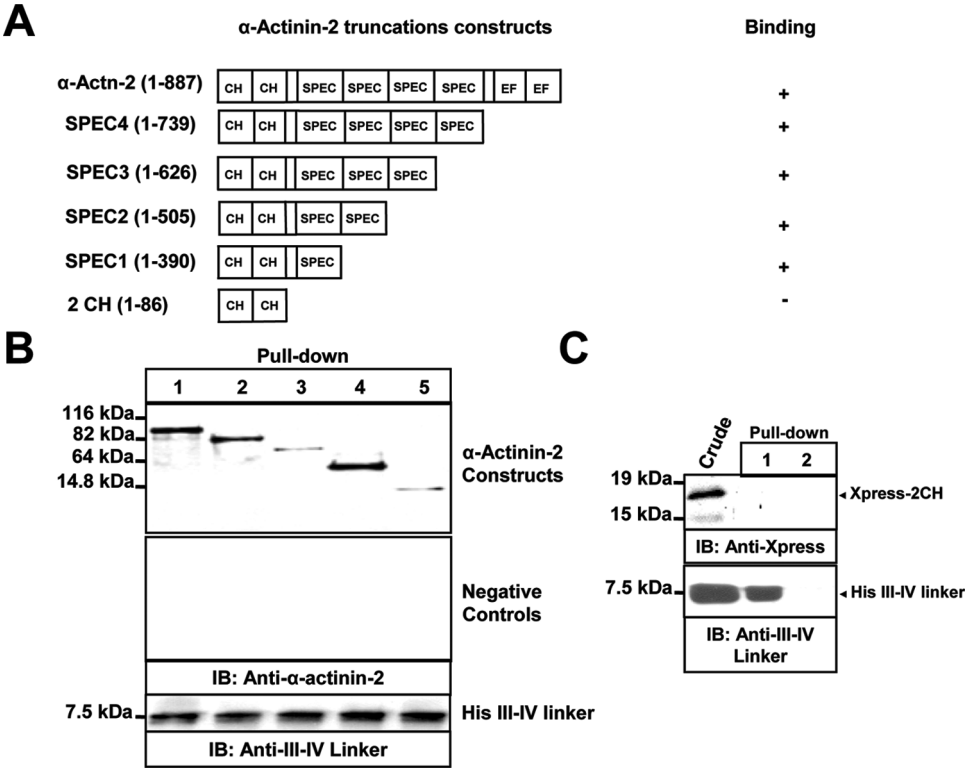

FIGURE 6: Spectrin-like repeat motifs of α-actinin-2 were required for the interaction with the $Na_v1.5$/LIII−IV protein. (A) Schematic representation of full-length α-actinin-2 and the C-terminally truncated α-actinin-2 specific fragments used to map the α-actinin-2 binding sites for LIII−IV. α-Actinin-2 domains are abbreviated as follows: 2 CH, calponin homology domain; SPEC1−SPEC4, SRM; EF, EF-hand domain. The numbers refer to the amino acid residues in the α-actinin-2 constructs. The binding or lack of binding of the various α-actinin-2 segments to LIII−IV, as shown in panel B, is indicated by a plus or minus sign, respectively. (B and C) His pull-down assays. tsA201 cells transiently expressing full-length α-actinin-2 (positive control, lane 1) or C-terminally truncated α-actinin-2 fragments [the SPEC4 domain (lane 2), the SPEC3 domain (lane 3), the SPEC2 domain (lane 4), the SPEC1 domain (lane 5), and the Xpress-tagged 2 CH domain (C, lane 1)] were incubated with either His_6-LIII−IV fusion protein prebound to Ni^{2+}-NTA beads or Ni^{2+}-NTA beads alone (negative control). Proteins bound to the His_6 fusion proteins or nickel beads were eluted and analyzed by Western blotting using an anti-α-actinin-2 (B, first panel) or anti-Xpress tag (C, first panel) antibody. These experiments were repeated three times with similar results.

SDS−PAGE and transferred to PDVF membranes. The blots were then incubated with anti-α-actinin-2 or anti-LIII−IV antibodies. As expected, the His_6-LIII−IV fusion protein successfully pulled down α-actinin-2 (lane 3), whereas no binding was observed with nickel beads alone (negative control, lane 4). The results of the His pull-down assays were in agreement with the overlay results and also showed that there was a direct interaction between α-actinin-2 and LIII−IV *in vitro*.

The Spectrin-like Repeat Motifs Are Required for the Interaction with the $Na_v1.5$/LIII−IV Protein. α-Actinin-2 contains two actin-binding domains (2 CH), four SRM (SPEC1−SPEC4), and an EF. To gain a more precise picture of the LIII−IV binding region of α-actinin-2, we generated five α-actinin-2 C-terminal truncation constructs (Figure 6A) and examined their ability to interact with the His_6-LIII−IV fusion protein using His pull-down assays. As shown in Figure 6B, the four SRM constructs (SPEC1−SPEC4), but not the two CH constructs (Figure 6C, top panel, lane 1), efficiently interacted with the His_6-LIII−IV fusion protein prebound to nickel beads (Figure 6C, top panel, lanes 2−5). Moreover, there was no significant association between the α-actinin-2 truncated contruct derivatives and the nickel beads alone (negative control) (Figure 6B, bottom panel, and Figure 6C, top panel, lane 2). These findings suggested that the central rod domain (amino acids 87−739), or at least one SRM (amino acids 87−390), of α-actinin-2 is essential for binding to LIII−IV. Interestingly, the central rod domain is also important for binding of α-actinin-2 to other ions channels such as NMDA receptors (*22*).

α-Actinin-2 and $Na_v1.5$ Colocalize in Human Cardiac Muscle Tissue. We used indirect double-label immunofluorescence and confocal microscopy to determine whether these two proteins colocalize (Figure 7). A series of 0.45 μm confocal optical serial sections showed that $Na_v1.5$ has a similar striated expression pattern in myocytes (Figure 7A,D), some diffuse intracell and surface labeling, and, occasionally, a dotted pattern outlining the striations, whereas the α-actinin-2 staining revealed, as expected, a striated pattern corresponding to sarcomeric Z-lines (Figure 7B,E). In the merged images, the striations and dots corresponding to $Na_v1.5$ [Figure 7C,F (yellow)] demonstrate that $Na_v1.5$ colocalized with α-actinin-2 along certain portions of the Z-lines. This is a further confirmation by the quatification of immunostaining of colocalization. A portion of 22 myocytes from 12 confocal images were used to quatify the colocalization of $Na_v1.5$ and α-actinin-2. The average colocalization coefficients were 0.45 ± 0.12 and 0.65 ± 0.14 for the green ($Na_v1.5$) and red channels (α-actinin-2), respectively. This suggests that 45% of $Na_v1.5$ staining colocalizes with α-actinin-2, while 65% of the α-actinin-2 signal colocalizes with $Na_v1.5$. To determine the degree of nonspecific binding, cardiomyocytes were incubated with a secondary antibody alone. Interestingly, no signal above background was detected, suggesting that the co-immunodetection is indeed specific (Figure 7G−I).

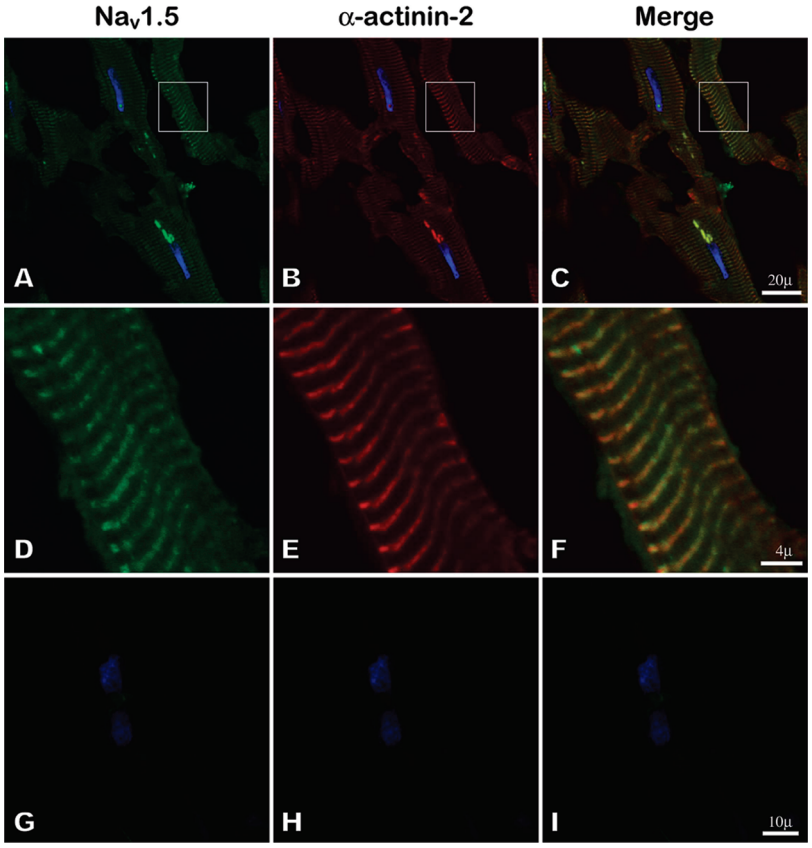

FIGURE 7: Na$_v$1.5 and α-actinin-2 colocalized in human cardiac tissue. Confocal microscopic examination of 0.45 μm sections of a human cardiac ventricle autopsy section stained with anti-Na$_v$1.5 (green in panels A, C, D, and F) and anti-α-actinin-2 4B antibodies (red in panels B, C, E, and F). Nuclei are stained with DAPI (blue) in all images. Merged images (C and F) show yellow striations, confirming the colocalization of α-actinin-2 and Na$_v$1.5 at Z-lines. Panels D−F are higher magnifications of the boxed regions. The rod-shaped structures in panels A−C fluoresced at all wavelengths and were also seen in unstained sections. They represent lipofuscin deposits in this autopsy specimen from an aged individual. Panels G−I show cardiomyocytes that were incubated with the secondary antibody alone. This experiment was performed three times with similar results.

α-*Actinin-2 Interacts with Other Sodium Channel Isoforms in Cyto and in Vivo*. The high degree of conservation of the LIII−IV polypeptide sequence among different tissues (*23*) and the presence of α-actinin-2 in skeletal muscle and the brain (*24*) suggest that α-actinin-2 may also interact with sodium channels expressed in these tissues. To verify this hypothesis, we performed immunoprecipitation experiments *in vivo* and *in cyto*. Mouse skeletal muscle protein extracts were immunoprecipitated with either an anti-LIII−IV polyclonal antibody [Figure 8A (IP, 1)] or with control preimmune IgG [Figure 8A (IP, 2)]. Bound proteins were detected by Western blotting using an anti-α-actinin-2 or anti-LIII−IV antibody. α-Actinin-2 protein was efficiently precipitated by the anti-LIII−IV antibody (Figure 8A, middle panel, lane 1) but not by the negative control serum (Figure 8A, middle panel, lane 2). Since the Na$_v$1.4 channel is strongly expressed in adult skeletal muscle (*25*), the endogenous adult skeletal muscle sodium channel immunoprecipitated with α-actinin-2 is most likely Na$_v$1.4. Interestingly, like α-actinin-2, α-actinin-3 is also expressed in skeletal muscle, where it forms heterodimers with α-actinin-2 (*19*). Because of this, we decided to explore a putative interaction between α-actinin-3 and skeletal sodium channels. Skeletal muscle samples were immunoprecipitated with an anti-LIII−IV antibody, and the blot was probed with anti-α-actinin-3 antibody. α-Actinin-3 was immunoprecipitated by the anti-LIII−IV antibody (Figure 8A, bottom panel, lane 1). These results demonstrated that α-actinin-2 and α-actinin-3 interact with endogenous skeletal sodium channels and suggested that both may be involved in the same channel complex in skeletal muscle. The anti-LIII−IV antibody also precipitated α-actinin-2 from mouse brain tissue extract (Figure 8B, lane 1). However, more experiments with specific antibodies will be needed to determine which brain sodium channel isoform is involved in this interaction. Lastly, we also observed an interaction between Na$_v$1.8, a sensory neuron-specific sodium channel, and α-actinin-2 in a heterologous expression system (Figure II of the Supporting Information). Our findings thus demonstrate that α-actinin-2 interacts with other sodium channel isoforms in skeletal muscle and brain tissue.

α-*Actinin-2 Increases Sodium Current Density in a Mammalian Expression System*. To investigate the functional consequences of α-actinin-2 expression on Na$_v$1.5 channel gating, we used the patch-clamp technique in the whole-cell configuration (Figure 9). We measured whole-cell sodium currents in tsA201 cells transiently transfected with either Na$_v$1.5 and the β_1 subunit (control) or Na$_v$1.5 and the β_1 subunit coexpressed with α-actinin-2. As shown in Figure 9A, the maximum sodium current density measured at −30 mV (estimated by dividing the peak current value by the membrane capacitance, p*A*/p*F*) of the control was, on average, 68% higher ($p < 0.01$) than when it was coexpressed with α-actinin-2 (Figure 9B), despite the fact that coexpressing Na$_v$1.5 and the β_1 subunit with α-actinin-2 did not alter cell capacitance [12.94 ± 1.43 pF ($n = 6$) vs 16.69 ± 1.7 pF ($n = 6$); p = ns]. Steady-state activation and inactivation gating

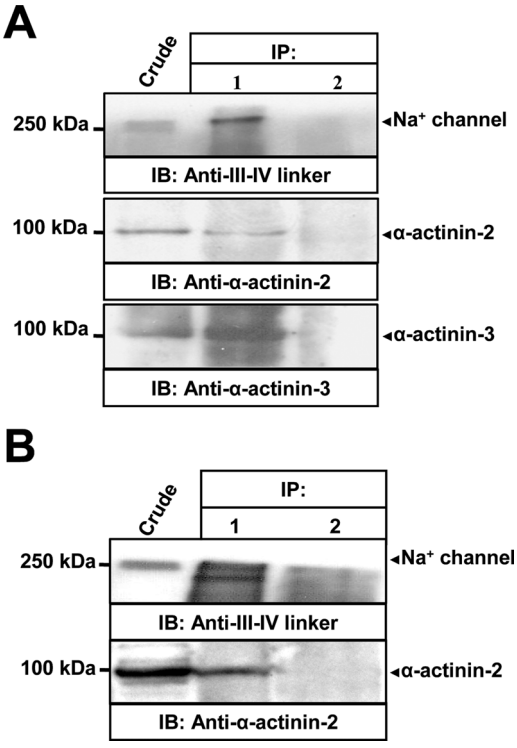

FIGURE 8: α-Actinin-2 interacted with endogenous sodium channels in mouse skeletal muscle and brain tissue. (A) Protein lysates extracted from adult mouse skeletal muscle cells were immunoprecipitated with anti-LIII−IV antibody (IP, 1) or preimmune IgG (negative control) (IP, 2). Signals were detected using anti-LIII−IV (top panel), anti-α-actinin-2 (middle panel), or anti-α-actinin-3 (bottom panel) antibody. The anti-LIII−IV antibody, but not the preimmune serum (middle and bottom panels, lane 2), immunoprecipitated α-actinin-2 and α-actinin-3 (middle and bottom panels, lane 1). α-Actinin-2 and α-actinin-3 specifically associated with skeletal muscle sodium channels *in vivo*. (B) Similarly, soluble sodium channel proteins extracted from adult mouse brain were immunoprecipitated with the anti-LIII−IV antibody (IP, 1) or rabbit preimmune IgG negative control (IP, 2), and the blots were probed with the anti-LIII−IV antibody (top panel) or the anti-α-actinin-2 antibody (bottom panel). α-Actinin-2 bound to endogenous sodium channels in mouse brain tissue. Aliquots of total cell extracts (Crude) were also loaded on the gel to serve as a positive control for the Western blotting. This experiment was performed three times with similar results.

properties were evaluated using the pulse protocols shown in the insets of Figure 10A,B. Neither the activation kinetics (Figure 10A; $V_{1/2act} = -49.60 \pm 2.13$ mV ($n = 6$) versus -51.40 ± 2.08 mV ($n = 6$), p = ns) nor the inactivation kinetics (Figure 10B; $V_{1/2act} = -101.85 \pm 2.32$ mV ($n = 6$) versus -102.47 ± 2.78 mV ($n = 6$), p = ns) of $Na_v1.5$ were altered by the coexpression with α-actinin-2. In conclusion, these results clearly showed that α-actinin-2 increases whole-cell $Na_v1.5$ currents.

α-Actinin-2 Increases the Level of Cell Surface Expression of $Na_v1.5$. The electrophysiological data presented so far argue for an α-actinin-2-mediated increase in the number of functional $Na_v1.5$ channels on the cell surface. To determine whether α-actinin-2 overexpression increases the number of $Na_v1.5$ channels in the plasma membrane, we isolated cell surface proteins by protein biotinylation using a membrane-impermeant biotin ester (Figure 11). Proteins isolated by neutravidin resin affinity precipitation were separated by SDS−PAGE, transferred to PVDF membranes, and immunoblotted with anti-LIII−IV, anti-Na^+/K^+-ATPase α1 subunit, and anti-β-tubulin antibodies.

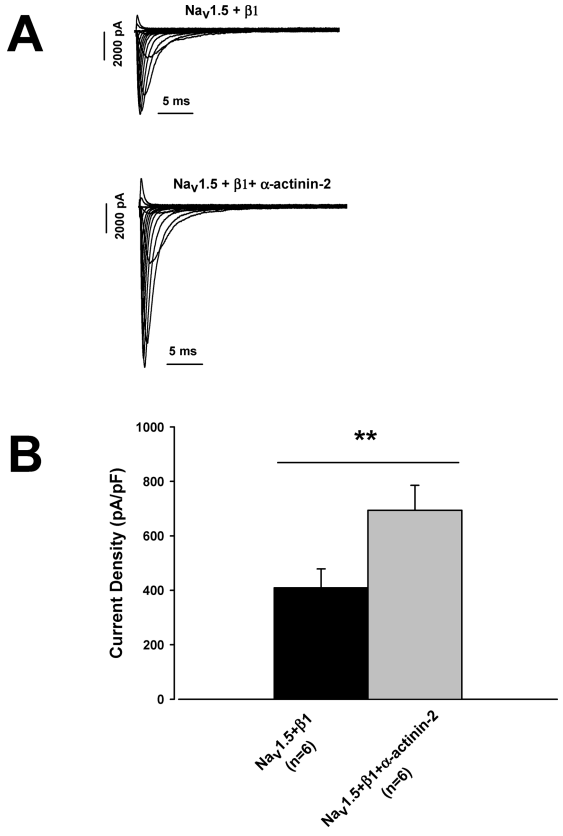

FIGURE 9: Overexpression of α-actinin-2 in tsA201 cells expressing $Na_v1.5$ increased sodium current densities. (A) Representative traces of currents recorded from control and cotransfected tsA201 cells transiently expressing $Na_v1.5+\beta_1$ (top) and $Na_v1.5+\beta_1+$α-actinin-2 (bottom). (B) Bar graph showing current densities at −30 mV in control cells ($Na_v1.5+\beta_1$) with current amplitudes of 409 ± 69.56 pA/pF ($n = 6$) and in cotransfected cells ($Na_v1.5+\beta_1+$ α-actinin-2) with current amplitudes of 693.80 ± 81.80 pA/pF ($n = 6$) (** $P < 0.01$).

The Na^+/K^+-ATPase α1 subunit was analyzed to ensure that equal amounts of protein extract (with and without α-actinin-2) were used (Figure 11, third panel). The absence of β-tubulin in the biotin-labeled samples indicated that the biotin reagent selectively labeled proteins in the plasma membrane (panel 4). As shown in Figure 11, overexpression of α-actinin-2 increased the amount of $Na_v1.5$ channel at the cell surface (panel 2, lanes 3 and 4, respectively) compared with an empty vector control (second panel, lane 1) or the $Na_v1.5$ channel expressed alone (panel 2, lane 2). These results also showed that the expression of the biotinylated $Na_v1.5$ channel depends on the amount of transfected α-actinin-2 cDNA. The total amount of $Na_v1.5$ was similar in the extracts (first panel 1). The quatification of the data shows a significant 4-fold increase in the level of $Na_v.5$ cell surface expression when contransfected with 5 μg of DNA encoding α-actinin-2 (Figure 11B). In contrast, the absence of β-tubulin in the streptavidin isolates indicated that biotin cannot penetrate the cell. These findings showed that α-actinin-2 mediates $Na_v1.5$ channel plasma membrane expression, which is consistent with the observation that coexpression of α-actinin-2 increases sodium channel densities.

DISCUSSION

We used a yeast two-hybrid screen to identify protein partners of the human cardiac sodium channel. We present evidence that

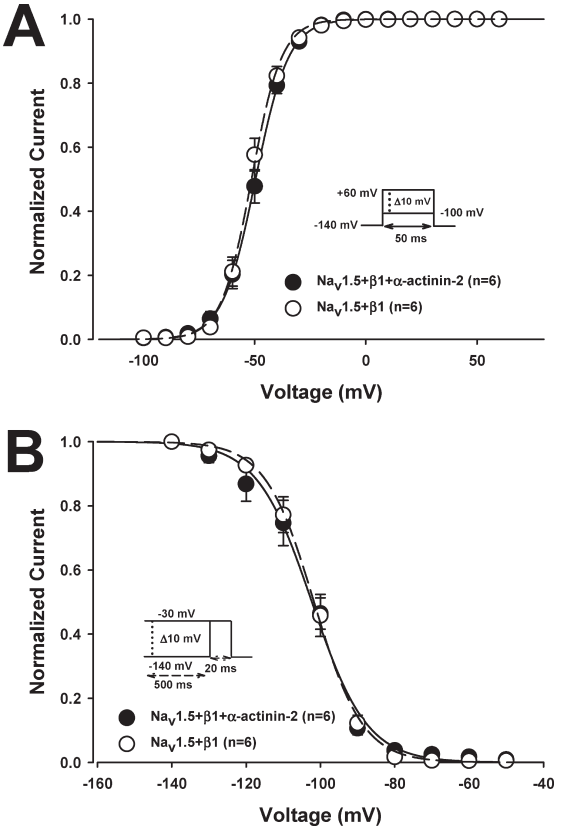

FIGURE 10: Overexpression of α-actinin-2 did not affect the steady-state activation and inactivation of $Na_v1.5$ channels. Steady-state activation (A) and inactivation (B) curves in tsA201 cells transiently cotransfected with $Na_v1.5$ and the β_1 subunit with or without α-actinin-2. Currents were elicited using 50 ms depolarization steps from −100 to 60 mV in 10 mV increments. The cells were held at a holding potential of −140 mV (see the inset for the protocol). The activation curves were constructed using the following Boltzmann equation: $G/G_{max} = 1/[1 + \exp(V_{1/2} - V)/k_v]$, where G is the measured conductance, G_{max} is the maximal conductance, $V_{1/2}$ is the voltage at which the channels are half-activated, and k_v is the slope factor. The fitting generated a $V_{1/2}$ of -49.60 ± 2.13 mV with a k_v of -6.45 ± 1.31 mV for $Na_v1.5$, β_1 subunit, and α-actinin-2 ($n = 6$) and a $V_{1/2}$ of -51.40 ± 2.08 mV with a k_v of -6.10 ± 1.45 mV for $Na_v1.5$ and β_1 subunit ($n = 6$). For the inactivation curves, the peak current (I) was normalized relative to the maximal value (I_{max}). The peak current amplitude was elicited by 20 ms test pulses to −30 mV after 500 ms prepulses at potentials ranging from −140 to −30 mV (see the inset for the protocol). The inactivation curves were fitted to the following Boltzmann equation: $I/I_{max} = a(1/\{1 + \exp[(V - V_{1/2})/k_v]\})$, where V is the membrane potential during the prepulse, $V_{1/2}$ is the voltage at which the channels are half-inactivated, and k_v is the slope factor. The fitting generated a $V_{1/2}$ of -102.47 ± 2.78 mV with a k_v of 6.42 ± 2.02 mV for $Na_v1.5$, β_1 subunit, and α-actinin-2 ($n = 6$) and a $V_{1/2}$ of -101.85 ± 2.32 mV with a k_v of 6.04 ± 2.11 mV for $Na_v1.5$ and β_1 subunit ($n = 6$).

α-actinin-2 specifically binds to the LIII−IV polypeptide *in vitro* and *in cyto*. Colocalization of $Na_v1.5$ and α-actinin-2 in the regions where T-tubules contact Z-lines in human cardiac ventricles and the ability of α-actinin-2 to modulate sodium current densities and cell surface expression of the channel in tsA201 cells suggest that the interaction is physiologically relevant.

Given the high degree of sequence identity (50%) among sodium channels (*26*), we were not surprised that α-actinin-2 also bound to other sodium channels such as $Na_v1.8$ and endogenous sodium channels from skeletal muscle and brain tissue. There are two sodium channel isoforms ($Na_v1.4$ and $Na_v1.5$) in skeletal

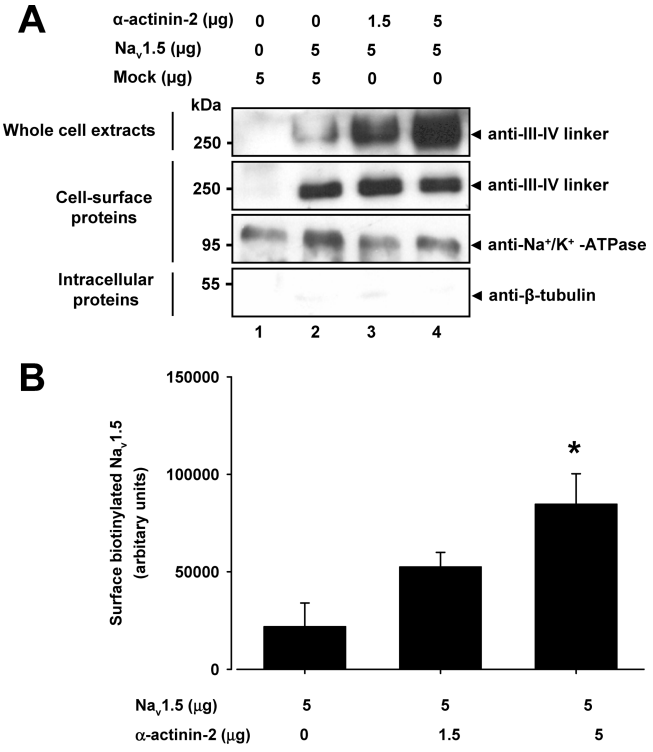

FIGURE 11: Coexpression of α-actinin-2 and $Na_v1.5$ increased the level of cell surface expression of $Na_v1.5$. (A) $Na_v1.5$ channels were transfected into tsA201 cells with empty vector (mock) or increasing amounts (1.5−5 g) of cDNA encoding α-actinin-2. Forty-eight hours later, the total membrane proteins were labeled with a membrane-impermeable biotinylation reagent and isolated membrane proteins were labeled with streptavidin beads. Channel immunoreactivity in the whole cell lysates (positive control, first panel) and in the streptavidin precipitates (second panel) was detected using an anti-LIII−IV antibody. Cell surface expression of $Na_v1.5$ in the presence of α-actinin-2 (second panel, lanes 3 and 4) and in the absence of α-actinin-2 (second panel, lane 1). The blots were also probed with anti-Na^+/K^+-ATPase α1 antibody as a cell surface protein marker (third panel) and with anti-β-tubilin antibody as a negative control (fourth panel). This experiment was repeated at least four times, and similar results were obtained. (B) Quantification of the data.

muscle. The $Na_v1.4$ channel is more strongly expressed in adult than in neonatal rat skeletal muscle, whereas the $Na_v1.5$ channel can be detected in neonatal skeletal muscle and after denervation of adult muscle (*27*, *28*). The endogenous skeletal sodium channel involved in the interaction with α-actinin-2 is thus most likely $Na_v1.4$. However, the functional significance of the α-actinin-2−sodium channel isoform interaction has yet to be determined in native tissue, where both are well expressed.

α-Actinin-2 belongs to the large family of spectrin-like proteins (*29*). There are four α-actinin genes, two nonskeletal muscle isoforms, α-actinin-1 and -4, and two skeletal muscle isoforms, α-actinin-2 and -3 (*10*), all of which share a general structure than can be divided into three functionally distinct domains [two highly conserved CH domains in the N-terminus that are necessary for actin binding, followed by four SRM that make up a central rod domain that is required for the antiparallel dimerization of α-actinin-2, and two carboxy-terminal EF-hand CaM domains (*11*)]. The SRM of α-actinin-2, which is the region that interacts with $Na_v1.5$, has been mapped. The structure of the central rod domain of actinin is a twisted antiparallel homodimer. The four SRM in this domain form tight dimer contacts and a rigid connection between two actin-binding domains positioned at the two ends of the actinin dimer. The SRM are

also important interaction sites for a number of structural and signaling proteins such as NMDA receptors, potassium channels ($K_v1.4$ and $K_v1.5$), the polycystin-2 channel, and the transient receptor potential polycystin 3 (TRPP3) (*13*, *16*, *22*, *30*).

Because of the high level of sequence identity between α-actinin isoforms, we looked at whether $Na_v1.5$ interacted with all the α-actinin isoforms. Interestingly, we found that α-actinin-1, α-actinin-3, and α-actinin-4 interacted with $Na_v1.5$ in a heterologous expression system. We also showed that skeletal muscle sodium channels interact with two skeletal muscle isoforms of α-actinin (α-actinin-2 and α-actinin-3) *in vivo*. The nonmuscle α-actinin isoforms (α-actinin-1 and -4), like α-actinin-2, have been implicated in the anchoring of other ion channels to the cytoskeleton. The interaction of α-actinin-1 with the $mGlu_{5b}$ receptor modulates the cell surface expression of the receptor. This is dependent on the binding of α-actinin-1 to the actin cytoskeleton (*31*). It has been suggested that α-actinin-4 may link acid-sensing ion channel 1a (ASIC1a) to a macromolecular complex in the postsynaptic membrane where it regulates ASIC1a activity (*32*). It thus appears that α-actinin isoforms play a dual role as a component of the actin cytoskeleton and as a molecule that targets and anchors receptors to the plasma membrane.

α-Actinin-2 and the $Na_v1.5$ Channel Colocalize in Human Cardiac Tissue. Our immunocytochemical experiments revealed a striated, occasionally dotted, staining pattern, which is consistent with localization at T-tubules, with additional diffuse staining within the sarcoplasm and at cell membranes similar to the distribution reported by others (*33*−*35*). The $Na_v1.5$-positive striations colocalized with α-actinin-2 positive Z-lines, indicating that the interaction between $Na_v1.5$ channels and α-actinin-2 likely occurs in regions where T-tubules contact Z-lines. In cardiomyocytes, α-actinin-2 is essentially localized at the Z-line (*24*). However, the precise localization of $Na_v1.5$ in cardiomyocytes is somewhat controversial. It is known that a pool of $Na_v1.5$ is localized at specialized cell−cell junctions or intercalated disks (*36*, *37*). The presence of $Na_v1.5$ in lateral membranes and T-tubules, however, is still a matter of discussion (*34*, *37*). It is interesting to note that $Na_v1.5$ interacts with dystrophin, which is predominantly localized in the transverse tubule/Z-line (*38*) but is not present in intercalated disks (*39*). The loss of dystrophin affected the expression levels of $Na_v1.5$, leading to a reduced sodium current density. Hence, the hypothesis that at least two pools of $Na_v1.5$ channels exist in the plasma membrane of cardiomyocytes cannot be excluded (*9*). The first pool would be localized in lateral membranes and would consist of dystrophin-associated proteins, whereas the second pool would be localized in the intercalated disks. Our results support this hypothesis and suggest that the localization of $Na_v1.5$ in the T-tubules appears to be dependent on its interaction with proteins such as α-actinin-2, dystrophin, syntrophin, and other PDZ domain proteins. Furthermore, the differential localization of $Na_v1.5$ channels in intercalated disks versus T-tubules is likely related to age. Kucera et al. (*40*) showed that $Na_v1.5$ is localized in nascent intercalated disks in neonatal cardiac myocytes, whereas Haufe et al. (*41*) reported that $Na_v1.5$ is expressed in the intercalated disks as well as at the Z-lines in cardiomyocytes isolated from 38-day-old mice (*42*). Interestingly, Haufe et al. (*41*) also observed that tetrodotoxin-sensitive $Na_v1.1$ in canine cells is mainly expressed in intercalated disks with only a faint Z-line distribution. Consequently, there may be additional species-specific roles for tetrodotoxin-sensitive sodium channel isoforms. As such, species differences must be taken into account when studying the cardiac distribution of $Na_v1.5$. With all this together, the precise localization of $Na_v1.5$ in cardiomyocytes is somewhat controversial. The use of distinct sources of antibodies, different species, and technical procedures might underlie such differences, although such controversies are still a matter of further discussion (*34*, *37*). Differentially localized sodium channels may have different physiological roles (*36*, *37*).

What Is the Functional Significance of the Interaction of α-Actinin-2 with the $Na_v1.5$ Channel? Patch-clamp experiments showed that the expression of α-actinin-2 in tsA201 cells transiently transfected with $Na_v1.5$ resulted in an average 68% increase in the whole-cell sodium current density. However, the biophysical properties of the channel were not altered, and only the channel density was increased. Cell surface biotinylation experiments clearly supported this finding and demonstrated that there is much more $Na_v1.5$ protein on the surface of tsA201 cells coexpressing α-actinin-2. Our findings are in agreement with the proposed mode of α-actinin-2 action on voltage-gated K^+ channels (*43*) and point to a model in which α-actinin-2 increases the number of $Na_v1.5$ channels and/or availability on the cell surface, which in turn causes an increase in sodium current densities. However, indirect effects mediated through other cell targets of α-actinin-2 cannot be excluded. α-Actinin-2-associated proteins such as dystrophin also interact with the C-terminus of $Na_v1.5$ and play an important role in the appropriate expression and function of the channel in T-tubule membranes (*9*, *44*). Interestingly, the C-terminus of $Na_v1.5$ has been reported to interact with the LIII−IV fusion protein and form a complex that stabilizes the inactivated gate-occluded channel (*45*). Through these multiple interactions, α-actinin-2 may act together with dystrophin to ensure the proper localization and stabilization of $Na_v1.5$ channels in these regions. The absence of dystrophin in mdx^{5cv} cardiomyocytes significantly decreases sodium current densities and $Na_v1.5$ protein levels, whereas $Na_v1.5$ mRNA levels remain unchanged (*9*). We also observed a reduced level of expression of $Na_v1.5$ protein in mdx^{5cv} cardiomyocytes (data not shown). Conversely, the absence of dystrophin had no apparent effect on the cell expression of α-actinin-2. Likewise, the loss of dystrophin has been reported to modify the expression of sodium channels in skeletal muscle (*46*), while the tissue distribution of α-actinin-2 is unaffected (*47*). Most importantly, the expression in mdx mice of a chimeric microdystrophin transgene containing the four SRM of α-actinin-2 has been shown to ensure the correct assembly and localization of the dystrophin−glycoprotein complex in the sacrolemma at levels approximately equal to those associated with full-length dystrophin and to provide some protection from contraction-induced injury (*48*). One interpretation of these results is that α-actinin-2 may replace dystrophin when it is missing. Lastly, our findings support the notion that α-actinin-2 may be involved in the proper expression of $Na_v1.5$ by anchoring the channel at the cell membrane, making it less likely to be internalized and subsequently degraded. However, we cannot rule out the possibility of another indirect mechanism involving an α-actinin-2-associated protein complex containing dystrophin.

Do Changes in the Expression Level of $Na_v1.5$ Alter Cardiac Function? Changes in the sodium current densities and cell surface expression of $Na_v1.5$ are important determinants of the clinical phenotype of some cardiac disorders such as in Brugada syndrome (*49*, *50*). A significant increase in sodium current densities has been observed in cardiomyocytes from

guinea pigs with cardiac hypertrophy and failure (*51*), while a decrease in the level of membrane expression of $Na_v1.5$ has been observed in a dog model of atrial fibrillation (*49*, *50*). Similarly, Baba et al. (*52*) showed that dog cardiomyocytes isolated from infarcted zones have reduced sodium current densities associated with a marked loss of $Na_v1.5$ staining in T-tubules. In contrast, $Na_v1.5$ staining was unaffected in the intercalated disks. It is tempting to speculate that α-actinin-2 is involved in this phenomenon. Recently, two studies showed that a loss of function mutation in the $Na_v1.5$ gene leads to dilated cardiomyopathy and atrial fibrillation in humans (*2*, *53*). Interestingly, α-actinin-2 mutations have also been associated with dilated cardiomyopathy (*54*). It would thus be interesting to analyze α-actinin-2 expression levels in pathological states and determine how α-actinin-2 mutations affect the expression and function of $Na_v1.5$ and lead to similar cardiac diseases. Further experiments exploring the physiological role of α-actinin-2 *in vivo* in mammalian myocardia are warranted. Resolving these issues will likely provide more insights into its role and its relevance in myocardial function and may provide interesting targets for new therapeutic strategies for treating lethal arrhythmias associated with $Na_v1.5$.

In conclusion, this study suggests that α-actinin-2 can promote or stabilize the targeting of the $Na_v1.5$ channel at specific subcellular membrane domains by interacting with the channel directly and/or indirectly through α-actinin-2-associated proteins or a yet to be discovered adaptor protein.

SUPPORTING INFORMATION AVAILABLE

Table I and Figures I and II. This material is available free of charge via the Internet at http://pubs.acs.org.

REFERENCES

1. George, A. L., Jr. (2005) Inherited disorders of voltage-gated sodium channels. *J. Clin. Invest. 115*, 1990–1999.
2. McNair, W. P., Ku, L., Taylor, M. R., Fain, P. R., Dao, D., Wolfel, E., and Mestroni, L. (2004) SCN5A mutation associated with dilated cardiomyopathy, conduction disorder, and arrhythmia. *Circulation 110*, 2163–2167.
3. Rougier, J. S., van Bemmelen, M. X., Bruce, M. C., Jespersen, T., Gavillet, B., Apothéloz, F., Cordonier, S., Staub, O., Rotin, D., and Abriel, H. (2005) Molecular Determinants of Voltage-Gated Sodium Channel Regulation by the Nedd4/Nedd4-like Proteins. *Am. J. Physiol. 288*, C692–C701.
4. McEwen, D. P., Meadows, L. S., Chen, C., Thyagarajan, V., and Isom, L. L. (2004) Sodium channel $\beta 1$ subunit-mediated modulation of Nav1.2 currents and cell surface density is dependent on interactions with contactin and ankyrin. *J. Biol. Chem. 279*, 16044–16049.
5. Fahmi, A. I., Patel, M., Stevens, E. B., Fowden, A. L., John, J. E., III, Lee, K., Pinnock, R., Morgan, K., Jackson, A. P., and Vandenberg, J. I. (2001) The sodium channel β-subunit SCN3b modulates the kinetics of SCN5a and is expressed heterogeneously in sheep heart. *J. Physiol. 537*, 693–700.
6. Zimmer, T., Biskup, C., Bollensdorff, C., and Benndorf, K. (2002) The $\beta 1$ subunit but not the $\beta 2$ subunit colocalizes with the human heart Na^+ channel (hH1) already within the endoplasmic reticulum. *J. Membr. Biol. 186*, 13–21.
7. Lemaillet, G., Walker, B., and Lambert, S. (2003) Identification of a conserved ankyrin-binding motif in the family of sodium channel α subunits. *J. Biol. Chem. 278*, 27333–27339.
8. Mohler, P. J., Rivolta, I., Napolitano, C., Lemaillet, G., Lambert, S., Priori, S. G., and Bennett, V. (2004) Nav1.5 E1053K mutation causing Brugada syndrome blocks binding to ankyrin-G and expression of Nav1.5 on the surface of cardiomyocytes. *Proc. Natl. Acad. Sci. U.S.A. 101*, 17533–17538.
9. Gavillet, B., Rougier, J. S., Domenighetti, A. A., Behar, R., Boixel, C., Ruchat, P., Lehr, H. A., Pedrazzini, T., and Abriel, H. (2006) Cardiac sodium channel Nav1.5 is regulated by a multiprotein complex composed of syntrophins and dystrophin. *Circ. Res. 99*, 407–414.
10. Takada, F., and Beggs, A. H. (2002) α-Actinins. In Encyclopedia of Molecular Medicine (Creighton, T. E., Ed.) pp 122−127, John Wiley & Sons, Inc., New York.
11. Beggs, A. H., Byers, T. J., Knoll, J. H., Boyce, F. M., Bruns, G. A., and Kunkel, L. M. (1992) Cloning and characterization of two human skeletal muscle α-actinin genes located on chromosomes 1 and 11. *J. Biol. Chem. 267*, 9281–9288.
12. Otey, C. A., and Carpen, O. (2004) α-Actinin revisited: A fresh look at an old player. *Cell Motil. Cytoskeleton 58*, 104–111.
13. Li, Q., Montalbetti, N., Shen, P. Y., Dai, X. Q., Cheeseman, C. I., Karpinski, E., Wu, G., Cantiello, H. F., and Chen, X. Z. (2005) α-Actinin associates with polycystin-2 and regulates its channel activity. *Hum. Mol. Genet. 14*, 1587–1603.
14. Schulz, T. W., Nakagawa, T., Licznerski, P., Pawlak, V., Kolleker, A., Rozov, A., Kim, J., Dittgen, T., Kohr, G., Sheng, M., Seeburg, P. H., and Osten, P. (2004) Actin/αactinin-dependent transport of AMPA receptors in dendritic spines: Role of the PDZ-LIM protein RIL. *J. Neurosci. 24*, 8584–8594.
15. Fedida, D., Maruoka, N. D., and Lin, S. (1999) Modulation of slow inactivation in human cardiac Kv1.5 channels by extra- and intracellular permeant cations. *J. Physiol. 515*, 315–329.
16. Djinovic-Carugo, K., Gautel, M., Ylanne, J., and Young, P. (2002) The spectrin repeat: A structural platform for cytoskeletal protein assemblies. *FEBS Lett. 513*, 119–123.
17. Gellens, M. E., George, A. L., Jr., Chen, L. Q., Chahine, M., Horn, R., Barchi, R. L., and Kallen, R. G. (1992) Primary structure and functional expression of the human cardiac tetrodotoxin-insensitive voltage-dependent sodium channel. *Proc. Natl. Acad. Sci. U.S.A. 89*, 554–558.
18. Margolskee, R. F., McHendry-Rinde, B., and Horn, R. (1993) Panning transfected cells for electrophysiological studies. *BioTechniques 15*, 906–911.
19. Chan, Y. M., Tong, H. Q., Beggs, A. H., and Kunkel, L. M. (1998) Human skeletal muscle-specific α-actinin-2 and -3 isoforms form homodimers and heterodimers *in vitro* and *in vivo*. *Biochem. Biophys. Res. Commun. 248*, 134–139.
20. Chahine, M., Pilote, S., Pouliot, V., Takami, H., and Sato, C. (2004) Role of arginine residues on the S4 segment of the *Bacillus halodurans* Na^+ channel in voltage-sensing. *J. Membr. Biol. 201*, 9–24.
21. Virel, A., and Backman, L. (2004) Molecular evolution and structure of α-actinin. *Mol. Biol. Evol. 21*, 1024–1031.
22. Wyszynski, M., Kharazia, V., Shanghvi, R., Rao, A., Beggs, A. H., Craig, A. M., Weinberg, R., and Sheng, M. (1998) Differential regional expression and ultrastructural localization of α-actinin-2, a putative NMDA receptor-anchoring protein, in rat brain. *J. Neurosci. 18*, 1383–1392.
23. Hartmann, H. A., Tiedeman, A. A., Chen, S. F., Brown, A. M., and Kirsch, G. E. (1994) Effects of III-IV linker mutations on human heart Na^+ channel inactivation gating. *Circ. Res. 75*, 114–122.
24. Mills, M., Yang, N., Weinberger, R., Vander Woude, D. L., Beggs, A. H., Easteal, S., and North, K. (2001) Differential expression of the actin-binding proteins, α-actinin-2 and -3, in different species: Implications for the evolution of functional redundancy. *Hum. Mol. Genet. 10*, 1335–1346.
25. Trimmer, J. S., Cooperman, S. S., Agnew, W. S., and Mandel, G. (1990) Regulation of muscle sodium channel transcripts during development and in response to denervation. *Dev. Biol. 142*, 360–367.
26. Goldin, A. L., Barchi, R. L., Caldwell, J. H., Hofmann, F., Howe, J. R., Hunter, J. C., Kallen, R. G., Mandel, G., Meisler, M. H., Berwald-Netter, Y., Noda, M., Tamkun, M. M., Waxman, S. G., Wood, J. N., and Catterall, W. A. (2000) Nomenclature of voltage-gated sodium channels. *Neuron 28*, 365–368.
27. Goldin, A. L. (1999) Diversity of mammalian voltage-gated sodium channels. *Ann. N.Y. Acad. Sci. 868*, 38–50.
28. Kallen, R. G., Sheng, Z. H., Yang, J., Chen, L. Q., Rogart, R. B., and Barchi, R. L. (1990) Primary structure and expression of a sodium channel characteristic of denervated and immature rat skeletal muscle. *Neuron 4*, 233–242.
29. Sjoblom, B., Salmazo, A., and Djinovic-Carugo, K. (2008) α-Actinin structure and regulation. *Cell. Mol. Life Sci. 65*, 2688–2701.
30. Cukovic, D., Lu, G. W. K., Wible, B., Steele, D. F., and Fedida, D. (2001) A discrete amino terminal domain of Kv1.5 and Kv1.4 potassium channels interacts with the spectrin repeats of α-actinin-2. *FEBS Lett. 498*, 87–92.
31. Cabello, N., Remelli, R., Canela, L., Soriguera, A., Mallol, J., Canela, E. I., Robbins, M. J., Lluis, C., Franco, R., McIlhinney, J., and

Ciruela, F. (2007) Actin-binding protein α-actinin-1 interacts with the metabotropic glutamate receptor type 5b and modulates the cell surface expression and function of the receptor. *J. Biol. Chem. 282*, 12143–12153.
32. Schnizler, M. K., Schnizler, K., Zha, X. M., Hall, D. D., Wemmie, J. A., Hell, J. W., and Welsh, M. J. (2009) The cytoskeletal protein α-actinin regulates acid-sensing ion channel 1a through a C-terminal interaction. *J. Biol. Chem. 284*, 2697–2705.
33. Wagner, S., Dybkova, N., Rasenack, E. C. L., Jacobshagen, C., Fabritz, L., Kirchhof, P., Maier, S. K. G., Zhang, T., Hasenfuss, G., Brown, J. H., Bers, D. M., and Maier, L. S. (2006) Ca^{2+}/calmodulin-dependent protein kinase II regulates cardiac Na^+ channels. *J. Clin. Invest. 116*, 3127–3138.
34. Dominguez, J. N., de la Rosa, A., Navarro, F., Franco, D., and Aranega, A. E. (2008) Tissue distribution and subcellular localization of the cardiac sodium channel during mouse heart development. *Cardiovasc. Res. 78*, 45–52.
35. Qu, Y., Karnabi, E., Chahine, M., Vassalle, M., and Boutjdir, M. (2007) Expression of skeletal muscle $Na_V1.4$ Na channel isoform in canine cardiac Purkinje myocytes. *Biochem. Biophys. Res. Commun. 355*, 28–33.
36. Cohen, S. A. (1996) Immunocytochemical localization of rH1 sodium channel in adult rat heart atria and ventricle. Presence in terminal intercalated disks. *Circulation 94*, 3083–3086.
37. Maier, S. K. G., Westenbroek, R. E., McCormick, K. A., Curtis, R., Scheuer, T., and Catterall, W. A. (2004) Distinct subcellular localization of different sodium channel α and *β* subunits in single ventricular myocytes from mouse heart. *Circulation 109*, 1421–1427.
38. Peri, V., Ajdukovic, B., Holland, P., and Tuana, B. S. (1994) Dystrophin predominantly localizes to the transverse tubule/Z-line regions of single ventricular myocytes and exhibits distinct associations with the membrane. *Mol. Cell. Biochem. 130*, 57–65.
39. Kaprielian, R. R., Stevenson, S., Rothery, S. M., Cullen, M. J., and Severs, N. J. (2000) Distinct patterns of dystrophin organization in myocyte sarcolemma and transverse tubules of normal and diseased human myocardium. *Circulation 101*, 2586–2594.
40. Kucera, J. P., Rohr, S., and Rudy, Y. (2002) Localization of sodium channels in intercalated disks modulates cardiac conduction. *Circ. Res. 91*, 1176–1182.
41. Haufe, V., Camacho, J. A., Dumaine, R., Gunther, B., Bollensdorff, C., von Banchet, G. S., Benndorf, K., and Zimmer, T. (2005) Expression pattern of neuronal and skeletal muscle voltage-gated Na^+ channels in the developing mouse heart. *J. Physiol. 564*, 683–696.
42. Haufe, V., Cordeiro, J. M., Zimmer, T., Wu, Y. S., Schiccitano, S., Benndorf, K., and Dumaine, R. (2005) Contribution of neuronal sodium channels to the cardiac fast sodium current INa is greater in dog heart Purkinje fibers than in ventricles. *Cardiovasc. Res. 65*, 117–127.
43. Maruoka, N. D., Steele, D. F., Au, B. P. Y., Dan, P., Zhang, X., Moore, E. D. W., and Fedida, D. (2000) α-Actinin-2 couples to cardiac Kv1.5 channels, regulating current density and channel localization in HEK cells. *FEBS Lett. 473*, 188–194.
44. Hance, J. E., Fu, S. Y., Watkins, S. C., Beggs, A. H., and Michalak, M. (1999) α-Actinin-2 is a new component of the dystrophin-glycoprotein complex. *Arch. Biochem. Biophys. 365*, 216–222.
45. Motoike, H. K., Liu, H., Glaaser, I. W., Yang, A. S. Y., Tateyama, M., and Kass, R. S. (2004) The Na^+ channel inactivation gate is a molecular complex: A novel role of the COOH-terminal domain. *J. Gen. Physiol. 123*, 155–165.
46. Ribaux, P., Bleicher, F., Couble, M. L., Amsellem, J., Cohen, S. A., Berthier, C., and Blaineau, S. (2001) Voltage-gated sodium channel (SkM1) content in dystrophin-deficient muscle. *Pfluegers Arch. 441*, 746–755.
47. Williams, M. W., and Bloch, R. J. (1999) Extensive but coordinated reorganization of the membrane skeleton in myofibers of dystrophic (mdx) mice. *J. Cell Biol. 144*, 1259–1270.
48. Harper, S. Q., Hauser, M. A., DelloRusso, C., Duan, D., Crawford, R. W., Phelps, S. F., Harper, H. A., Robinson, A. S., Engelhardt, J. F., Brooks, S. V., and Chamberlain, J. S. (2002) Modular flexibility of dystrophin: Implications for gene therapy of Duchenne muscular dystrophy. *Nat. Med. 8*, 253–261.
49. Baroudi, G., Pouliot, V., Denjoy, I., Guicheney, P., Shrier, A., and Chahine, M. (2001) Novel mechanism for Brugada syndrome: Defective surface localization of an *SCN5A* mutant (R1432G). *Circ. Res. 88*, E78–E83.
50. Brugada, J., Brugada, R., and Brugada, P. (1998) Right bundle-branch block and ST-segment elevation in leads V_1 through V_3: A marker for sudden death in patients without demonstrable structural heart disease. *Circulation 97*, 457–460.
51. Ahmmed, G. U., Dong, P. H., Song, G., Ball, N. A., Xu, Y., Walsh, R. A., and Chiamvimonvat, N. (2000) Changes in Ca^{2+} cycling proteins underlie cardiac action potential prolongation in a pressure-overloaded guinea pig model with cardiac hypertrophy and failure. *Circ. Res. 86*, 558–570.
52. Baba, S., Dun, W., Cabo, C., and Boyden, P. A. (2005) Remodeling in cells from different regions of the reentrant circuit during ventricular tachycardia. *Circulation 112*, 2386–2396.
53. Olson, T. M., Michels, V. V., Ballew, J. D., Reyna, S. P., Karst, M. L., Herron, K. J., Horton, S. C., Rodeheffer, R. J., and Anderson, J. L. (2005) Sodium channel mutations and susceptibility to heart failure and atrial fibrillation. *J. Am. Med. Assoc. 293*, 447–454.
54. Mohapatra, B., Jimenez, S., Lin, J. H., Bowles, K. R., Coveler, K. J., Marx, J. G., Chrisco, M. A., Murphy, R. T., Lurie, P. R., Schwartz, R. J., Elliott, P. M., Vatta, M., McKenna, W., Towbin, J. A., and Bowles, N. E. (2003) Mutations in the muscle LIM protein and α-actinin-2 genes in dilated cardiomyopathy and endocardial fibroelastosis. *Mol. Genet. Metab. 80*, 207–215.